

Oxygen Isotope Data of Winter Water in the Western Weddell Sea: Preliminary Results

BOO-KEUN KHIM, BYONG-KWON PARK¹ AND SUNG-HO KANG¹

Research Institute of Oceanography, Seoul National University, Seoul 151-742, Korea

¹*Polar Research Center, Korea Ocean Research and Development Institute, Ansan 420-600, Korea*

In the western Weddell Sea, winter mixed layer is characterized by near-freezing temperature and higher salinity due to brine injection through sea-ice formation. This layer becomes Winter Water being capped by warmer and less saline Antarctic Surface Water during the sea-ice melting season. In this study, Winter Water was preliminarily identified by the oxygen isotopic compositions. The $\delta^{18}\text{O}$ values of Winter Water show the progressively increasing trend from south to north in the study area. It presumably reflects the enhanced mixing with Antarctic Surface Water due to the extent of influence by low $\delta^{18}\text{O}$ value of sea-ice/glacier meltwater. Correlations between salinity and $\delta^{18}\text{O}$ values of seawater can be used to more generally characterize Winter Water with a view to identification. However, the prediction on the degree of mixing from these relationships needs more detailed isotope data, although this study allows the oxygen isotopic composition of seawater as a tracer to identify the water mass.

INTRODUCTION

Classically, surface process of sea-ice formation over the continental shelf leads to bottom water production, raising the increase of salinity and density through a net brine release to a point where dense waters sink to the bottom (Brenneckè, 1921; Mosby, 1934). Much attention has been paid to the Antarctic Ocean, specially the Weddell Sea, due to the crucial site for the bottom water formation (AABW: Antarctic Bottom Water) (e.g., Gordon, 1988). Concerning on the global climate system, AABW in the Weddell Sea plays a significant role in transferring heat and influencing profoundly on the abyssal seawater properties (Killworth, 1983; Gordon, 1988).

The circulation pattern in the Weddell Sea is characterized by a cyclonic gyre, called as Weddell Gyre (WG). WG is bordered by the Antarctic continent on the south, by the Antarctic Peninsula on the west, and by the Scotia Ridge on the north, and extends as far east as 20 to 30°E (Deacon, 1979; Bagriantsev *et al.*, 1989; Orsi *et al.*, 1993). Along its eastern boundary, WG advects warm and saline Circumpolar Deep Water (CDW) from the Antarctic Circumpolar Current into the Weddell Sea (Foldvik *et al.*, 1985; Whitworth and Nowlin, 1987). The southern part of WG occupies the narrow but intense Antarctic Coastal Current flowing westward

and transporting relatively warm water onto the southwestern and western shelves (Fahrbach *et al.*, 1994). In contrast, the western and northern parts are significantly cold and fresh, reflecting the locally modified water flowing out of the Weddell Sea (Gordon, 1971; Carmack and Foster, 1974).

Various kinds of conservative and nonconservative tracers have been recently used along with the temperature and salinity to investigate the formation and circulation of bottom waters in the Weddell Sea (Weiss *et al.*, 1979; Jacob *et al.*, 1985; Schlosser *et al.*, 1991; Frew *et al.*, 1995; Mensch *et al.*, 1997). The oxygen isotopic composition of seawater has been known as a conservative tracer to complement temperature and salinity data (Epstein and Mayeda, 1953; Craig and Gordon, 1965; among others). Evaporation/precipitation processes are the main control of isotopic variation in the hydrological cycle, but sea-ice formation causes almost little effect (Tan and Strain, 1980; Ostlund and Hut, 1984). In addition, the mixing of water masses with different oxygen isotopic compositions results in another pathway to alter seawater $\delta^{18}\text{O}$ values (Fairbanks, 1982; Khim and Krantz, 1996; Khim *et al.*, 1997). Thus, the oxygen isotope ratios of seawater can be considered as an important tracer to characterize the seawater property even in the condition of sea-ice formation and melting.

Attention of this study is drawn to the sections

for the upper 500 m in the western Weddell Sea. We, thus, report the preliminary oxygen isotope data of seawater in the upper 200 m only. The objective of this paper is, based on the oxygen isotope dataset, to exploit the potential for the usefulness of isotope tracer for studies that characterize Winter Water in the western Weddell Sea. Greater emphasis is placed on presenting a comprehensive conservative data of seawater oxygen isotope to promote the better identification of Winter Water.

MATERIALS AND METHODS

A hydrographic survey was carried out in the austral summer of 1994/1995 aboard R/V *Yuhz-morgeologya* in the western Weddell Sea during the 8th Korea Antarctic Research Program of the Korea Ocean Research and Development Institute (Fig. 1). Vertically continuous profiles of temperature and salinity were obtained during each hydrocast from the two north-south transect lines comprising fourteen stations using a Sea-Bird Seacat conductivity-temperature-depth (CTD) recorder; seawater samples for oxygen isotope analyses were drawn from Niskin bottles mounted on the CTD rosette at discrete water levels for the upper 200 m of water depths. All the seawater samples were stored in 20-mL glass bottles with tight seals and returned to the laboratory for oxygen-18 analyses.

The oxygen isotopic compositions of seawater was determined by the standard technique of Epstein and Mayeda (1953). Each seawater sample of 2.0 ml was equilibrated at 25°C for 24 hours, after which the equilibrated carbon dioxide was introduced into a VG PRISM II dual inlet isotope mass spectrometer at the Korea Basic Science Institute. The original oxygen isotopic composition of the seawater was calculated by mass balance and calibrated against standard mean ocean water (SMOW). Approximately $\pm 0.1\%$ of precision is obtained through the repeated analyses of standard and samples. The oxygen isotopic values of seawater are presented in δ -notation, where $\delta^{18}\text{O}$ is the permil (‰) deviation of the $^{18}\text{O}/^{16}\text{O}$ ratios in a sample from that in SMOW (Craig, 1961) defined as

$$\delta^{18}\text{O} = \left[\frac{(^{18}\text{O}/^{16}\text{O})_{\text{sample}} - (^{18}\text{O}/^{16}\text{O})_{\text{SMOW}}}{(^{18}\text{O}/^{16}\text{O})_{\text{SMOW}}} \right] \times 1000$$

RESULTS AND DISCUSSION

Hydrography of two transects in the western Weddell Sea

Since the pioneering study by Deacon (1937), the water masses in the Weddell Sea can be conveniently differentiated on the basis of temperature

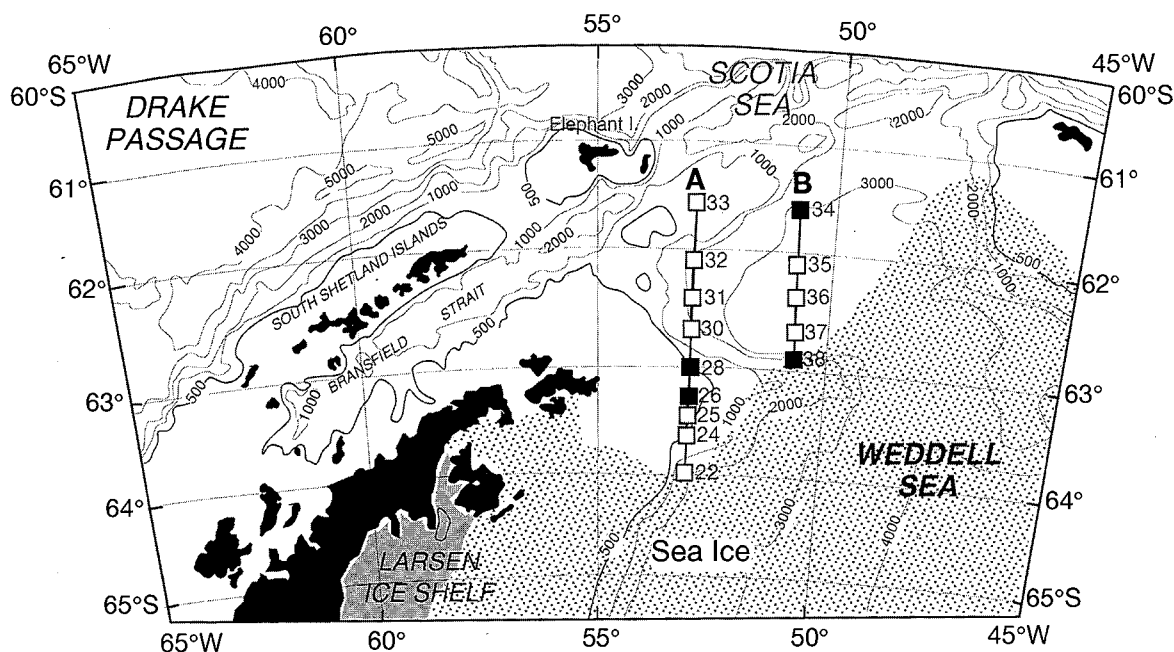


Fig. 1. Map showing bathymetry and two north-south transects (Transect A and Transect B) in the western Weddell Sea. Water depths are in meters. Open station=CTD with seawater sampling, closed station=just CTD hydrocasting.

and salinity data (Gordon, 1971; Gill, 1973; Carmack and Foster, 1974; Carmack, 1977 and others). Antarctic Surface Water (AASW) occupying the thin surface layer is warmed above freezing temperature and diluted by melting of sea ice in the austral summer. Winter Water (WW) underlies AASW and maintains the temperature minimum layer, i.e., a remnant of the winter mixed layer cooled to near the freezing point and enriched in salt by the formation of sea ice. Warm Deep Water (WDW) characterized by temperature and salinity maxima is located at mid-depth below a cold layer of WW. Below WDW is typically observed the cold bottom water mass of AABW.

The water masses of the upper part of the western Weddell Sea can be identified by TS diagrams and profiles of temperature and salinity (Fig. 2); both diagrams and profiles of two transects illustrate three distinct water masses (AASW, WW and

WDW) within the upper water column. Temperature and salinity of the water masses range from -1.83 to 0.54°C and from 33.85 to 34.70 psu (practical salinity units), respectively. The core representative of WW and WDW previously defined by Gordon (1971) and Carmack and Foster (1974) helps to identify the individual water masses. The pattern of TS diagram demonstrates that AASW varies widely, but exhibits the consistent and northward increase in temperature and salinity. This AASW is produced from the winter mixed layer by blending with freshwater from melted sea-ice/glacier and warming by solar radiation. WW is seen clearly and similarly in both transects, maintaining the temperature minimum. WDW is generally characterized by a temperature (0.5°C) and salinity (34.69 psu) maximum in the upper water column. The principal source of the warm and saline water and the detailed structure of WDW have been previously described by Gordon (1975).

Vertical distribution of temperature and salinity in the study area gives a clearer picture of water masses in the context of upper water column (Fig. 3). The top 30 to 50 m of the surface layer consists of AASW overlying WW (Fig. 3a and Fig. 3c). The surface layer includes water above a shallow (50–200 m) temperature minimum and salinities below 34.450 psu. At depths between 70 and 200 m the water column is characterized by lower temperatures. In winter the vertical distributions of potential temperature and salinity are practically homogeneous with temperature close to the freezing point of seawater, which approaches the critical value for the onset of cabbeling instability (Fofonoff, 1956; Foster, 1972). Thus, this temperature minimum layer corresponds to a remnant of wintertime convection which forms WW. Salinity increases gradually with water depth, maintaining the vertical stability in both transects (Fig. 3b and Fig. 3d). A relatively strong seasonal halocline is formed at 30–50 m with the lower salinity water in the surface layer separated from the water below.

Comparison on the vertical distribution of temperature and salinity between the two transects reflects different spatial structures within WW (Fig. 3). The thickness of WW in transect A is greater than that of transect B. The minimum temperature is lower in transect A than in transect B. Furthermore, the lower boundary of WW is more undulated and the northward extension of WW towards the Scotia Sea is less limited in transect A. The difference in

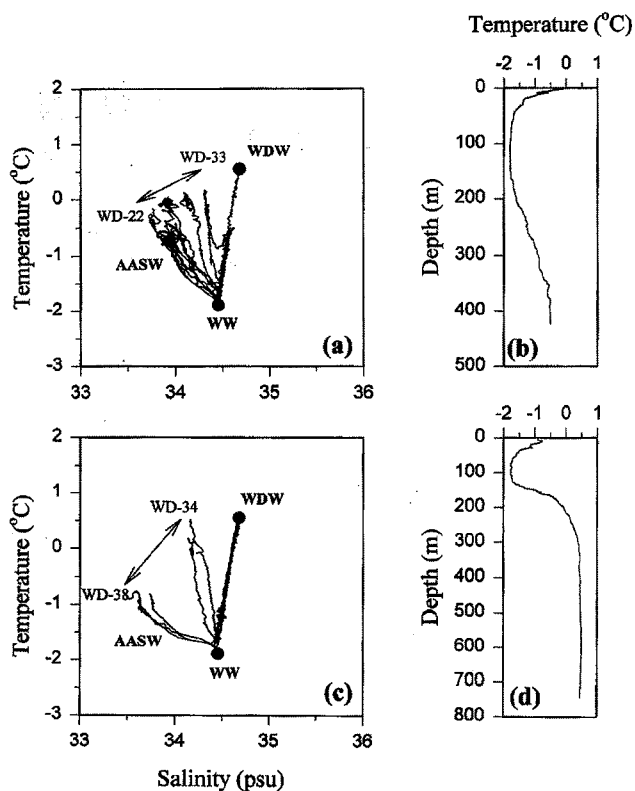


Fig. 2. (a) TS diagram of Transect A. (b) Temperature profile of station 28. (c) TS diagram of Transect B. (d) Temperature profile of station 36. AASW=Antarctic Surface Water, WW=Winter Water, WDW=Warm Deep Water. Note that the trend of AASW along the transects. Closed dots represent the core data of temperature and salinity for WW and WDW from Gordon (1971) and Carmack and Foster (1974).

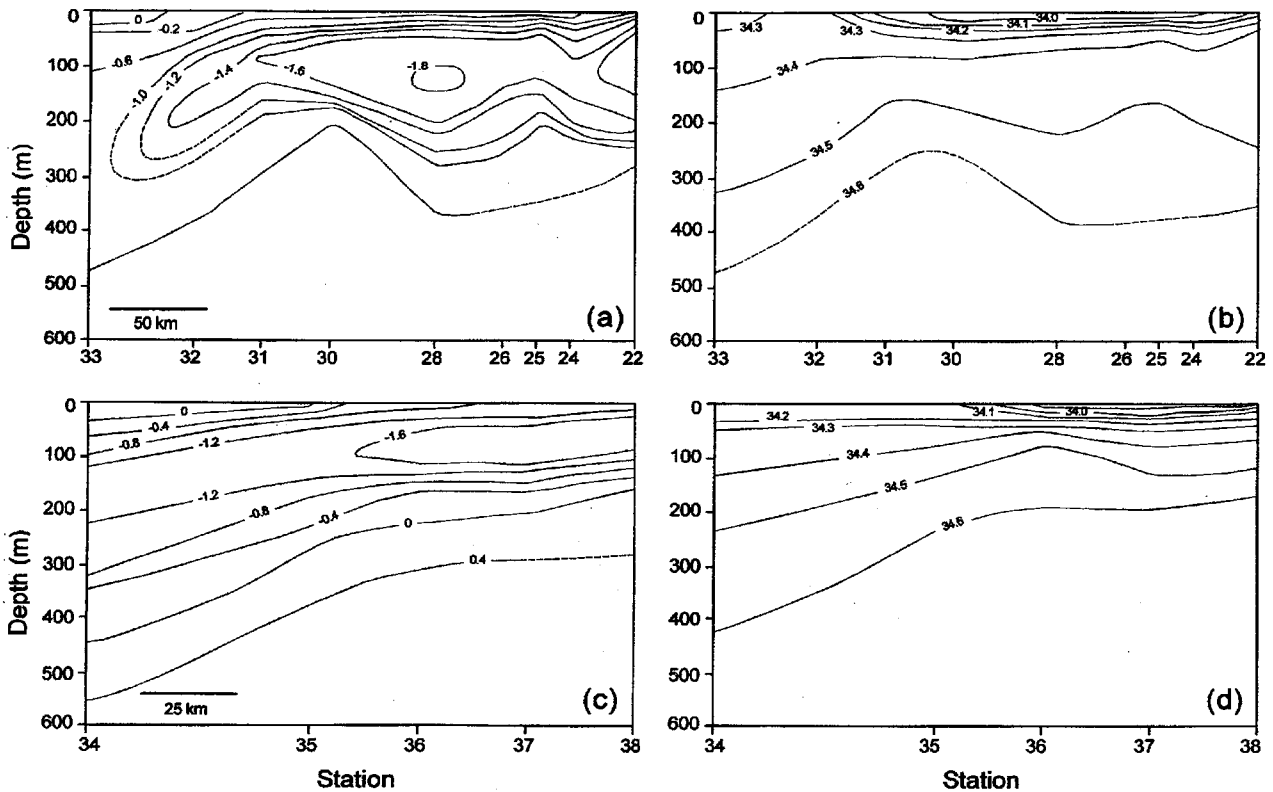


Fig. 3. Vertical distribution of temperature and salinity of two transects in the upper water masses of the western Weddell Sea. (a) Temperature of Transect A. (b) Salinity of Transect A. (c) Temperature of Transect B. (d) Salinity of Transect B. Refer the stations in Fig. 1.

WW structure between the two transects seems to be due to the thickness of the winter mixed layer, the degree of sea-ice melting by summer heating, wind intensity, and the proximity to the Bransfield Strait (Gordon and Nowlin, 1978; Gordon *et al.*, 1984; Carmack, 1986; Gordon and Huber, 1990).

Oxygen isotopic signature of Winter Water

Temperature and $\delta^{18}\text{O}$ values of seawater in the upper 200 m are plotted in Fig. 4. The two transects show a fairly wider range of temperatures and relatively small variations in $\delta^{18}\text{O}$ values. Considering the error range ($\pm 0.1\text{‰}$) of isotopic analyses, the variation of $\delta^{18}\text{O}$ values may be of little importance. Regardless, AASW of higher temperature in transect A seems to be divided into the northern and southern parts (solid line; Fig. 4a). The $\delta^{18}\text{O}$ value of AASW is a little greater in the northern part than in the southern part due presumably to the enhanced mixing with open ocean water that has been little influenced by sea-ice and/or glacier meltwater. Isotopic values of AASW in transect B are similarly

divided into north and south (solid line; Fig. 4b). The $\delta^{18}\text{O}$ values of subsurface seawater including WW are consistent in two transects, but those in transect A are correlated with temperature (dotted line; Fig. 4a). This may be the result of progressive mixing with water of lighter $\delta^{18}\text{O}$ value and higher temperature.

WW, formed by brine injection induced by sea-ice formation during winter (Mosby, 1934), lies below the seasonal halocline and is identified as a nearly isothermal temperature minimum layer (Fig. 3). Fig. 5 shows the distribution of $\delta^{18}\text{O}$ values in the upper water column. In transect A, the $\delta^{18}\text{O}$ values of 100-m and 150-m levels become gradually more positive from -0.44‰ to -0.21‰ (Fig. 5a). Such northward increase in $\delta^{18}\text{O}$ values can be attributed to enhanced mixing with AASW that has been little diluted by glacier meltwater. In contrast, in transect B, the $\delta^{18}\text{O}$ values of 150-m seawater are similarly increased from south to north, but the $\delta^{18}\text{O}$ values of 100-m level are invariant within the precision of the measurements (Fig. 5b). Such different trend in transect B may be due to the

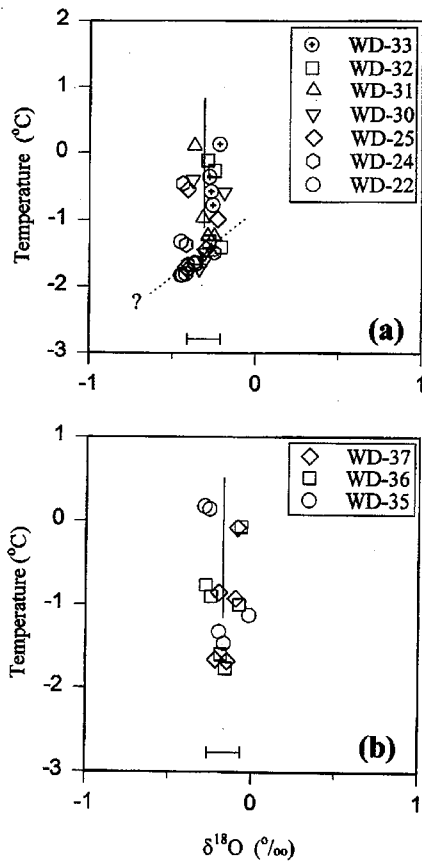


Fig. 4. Relationship between temperature and $\delta^{18}\text{O}$ values of seawater in the western Weddell Sea. (a) Transect A; (b) Transect B. The solid lines represent the division of AASW into the northern and southern parts. The dotted line in (a) may show the progressive mixing with water of lighter $\delta^{18}\text{O}$ value and higher temperature. The range of solid line on the horizontal axis is the error range for analytical precision.

degree of mixing with amounts of AASW. The $\delta^{18}\text{O}$ values corresponding to WW in transect A are lighter than those in transect B. This is also responsible for the regional difference of AASW effect. However, the quantitative estimate of mixing is difficult because of lack of data.

Correlations between salinity and $\delta^{18}\text{O}$ values in two transects are shown in Fig. 6, showing the simple mixing of the lower $\delta^{18}\text{O}$ and less saline waters with the higher $\delta^{18}\text{O}$ and more saline waters. In addition, the core of WW (34.40 psu, -0.25‰) from the result of Weiss *et al.* (1979) was compared with our data. The brine rejection during sea-ice formation leads to the higher salinity of remaining cold-temperature seawater equivalent to WW. However, it is well known that the fractionation of $\delta^{18}\text{O}$ in sea-ice equilibrated with seawater is so small

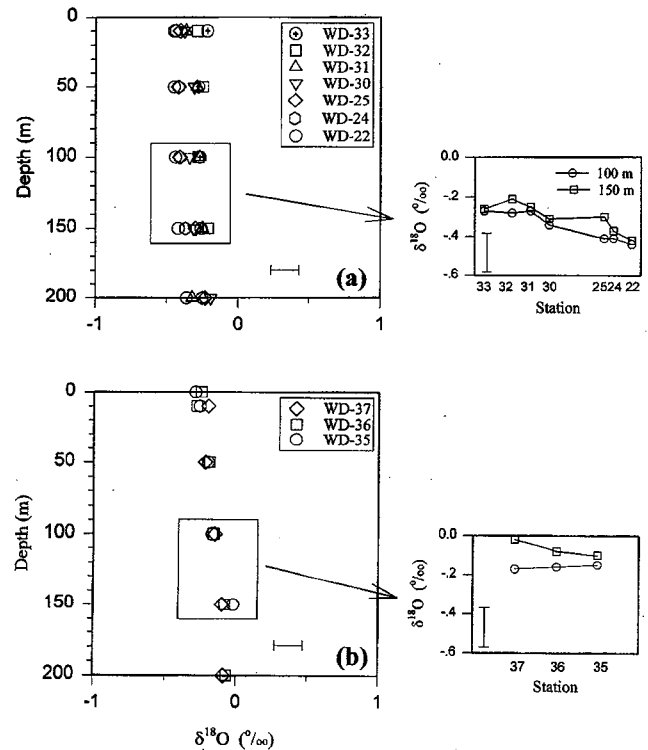


Fig. 5. Vertical distribution of $\delta^{18}\text{O}$ values of upper part of western Weddell Sea. (a) Transect A; (b) Transect B. The inset boxes illustrate the $\delta^{18}\text{O}$ variation of 100-m and 150-m level of seawater along the transects. The range of solid line in each graph is the error range for analytical precision.

(Lehmann and Siegenthaler, 1991) and the $\delta^{18}\text{O}$ value of glacier meltwater is much lower.

The correlation between salinity and $\delta^{18}\text{O}$ of seawater in transect A implies the complex mixing (Fig. 6a). All the seawater samples outside the inset box are under influence of the sea-ice meltwater, which causes the decrease in salinity with little change in isotopic composition. Of note are double mixings for the subsurface waters in the inset box. One is the typical mixing between isotopically lighter water and isotopically heavier seawater, on which the core composition of WW lies (solid line; Fig. 6a). The equation describing the mixing line is $\delta^{18}\text{O}=0.38\text{S}-13.2$ ($r^2=0.262$). The other mixing is represented by the dotted line towards WW (Fig. 6a). Such a mixing with steep slope presumably implies the relatively direct impact by the glacier meltwater, considering the lower salinities and $\delta^{18}\text{O}$ values. The variation of WW may be explained by the first mixing line. From the calculation, the $\delta^{18}\text{O}$ value of freshwater endmember in such mixing is apparently about -13‰ . However more detailed data are

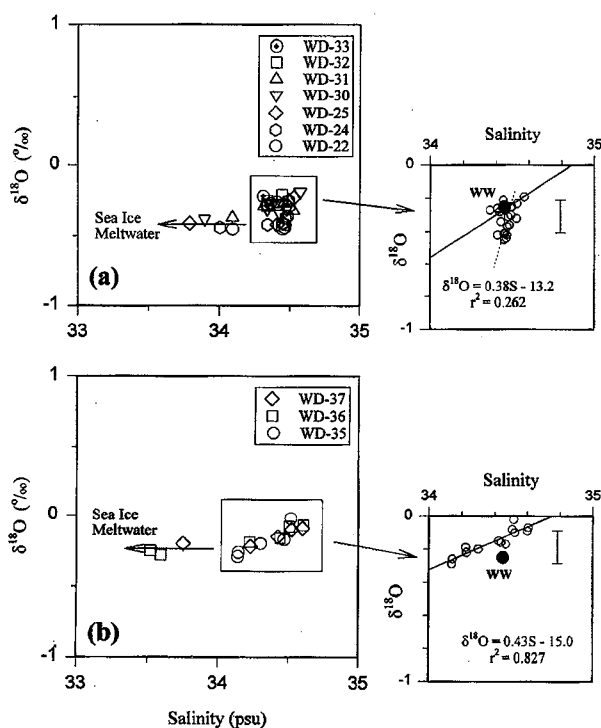


Fig. 6. Relationship between salinity and $\delta^{18}\text{O}$ values of seawater. (a) Transect A; (b) Transect B. The inset boxes depict the relationships between salinity and $\delta^{18}\text{O}$ values of the subsurface seawaters equivalent to WW. WW is from Weiss *et al.* (1979). Note the sea-ice meltwater effect. The range of solid line is the error range for analytical precision.

needed to verify this mixing because of the low correlation coefficient.

The relationship between $\delta^{18}\text{O}$ and salinity in transect B is a typical case of a two-component (freshwater and seawater) system (Fig. 6b). The effect of sea-ice meltwater can be factored out and the remaining $\delta^{18}\text{O}$ values and salinity produce the linearity described by a regression equation, $\delta^{18}\text{O} = 0.43S - 15.0$ ($r^2 = 0.827$). The slope and intercept in equation of transect B are accidentally similar to those in transect A, implying a degree of mixing is responsible for varying the characteristics of WW. The freshwater endmember for mixing lines of two transects ranges from -13 to -15‰ in spite of different correlation coefficients. The isotope property of glacial meltwater is characterized by extremely low $\delta^{18}\text{O}$ values and a measurement of $\delta^{18}\text{O}$ values of the snow and ice from the dry interior of the Antarctic continent ranges between -49 and -53‰ (Weiss *et al.*, 1979; Jacobs *et al.*, 1985). In the open ocean, surface water even in the Antarctic can be generally assumed to be around 0‰ of $\delta^{18}\text{O}$ values.

To make up for the mixing lines of WW in the study area, approximately 25 to 30% of glacier meltwater ultimately contributed to maintain the formation and mixing condition of WW. Thus, the currently available $\delta^{18}\text{O}$ data yields a significant $\delta^{18}\text{O}$ signal of WW, part of which may be contributed by the glacier meltwater. Nevertheless, too much positive $\delta^{18}\text{O}$ value of freshwater endmember can be justified, considering the open ocean system where the discharged glacier meltwaters are easily diluted by surface water.

SUMMARY

A hydrographic survey was undertaken in the western Weddell Sea performed by the 8th KARP (KORDI) in 1994/1995. Winter mixed layer resulted from surface process of homogenization during the winter time leads the preservation of Winter Water, a remnant of the winter surface layer cooled to near the freezing point and enriched in salt by the formation of sea ice. The occurrence of Winter Water in the study area is provided by temperature and salinity data. The preliminary oxygen isotopic data show that the $\delta^{18}\text{O}$ values of Winter Water increase progressively northward along the transects, suggesting the possible mixing with Antarctic Surface Water. The relationship between salinity and $\delta^{18}\text{O}$ values of seawater helps to prove potentially identifying Winter Water although the degree of mixing is difficult to predict yet due to the lack of isotopic data as well as the range of variation.

ACKNOWLEDGEMENTS

We appreciate the efforts of captain and crew of the R/V *Yuhzorgeology* during the 8th Korea Antarctic Research Program in 1994/1995. We also express our special thanks to Dr. H.I. Yoon (KORDI) and Mr. C.Y. Kang (KORDI) for hydro-casting and collecting seawater and to Dr. K.S. Lee (KBSI) for analyzing the oxygen isotopic composition. The first author acknowledges KOSEF for the support of the 1997/1998 Postdoctoral Fellowship. The manuscript was benefited from critical reviews by Dr. C.H. Kim (KORDI) and Dr. H.M. Lee (KORDI). The first author thanks to Dr. Lee W. Cooper (Oak Ridge National Lab) for his edition on the written expressions.

REFERENCES

- Bagriantsev, N.V., A.L. Gordon, and B.A. Huber, 1989. Weddell Gyre: Temperature maximum stratum. *J. Geophys. Res.*, **94**: 8331–8334.
- Brennecke, W., 1921. Die ozeanographischen Arbeiten der Deutschen Antarktischen Expedition, 1911–1912. *Arch. Deutsche Seewarte*, **39**: 1–216.
- Carmack, E.C., 1977. Water characteristics of the Southern Ocean south of polar front. In: A Voyage of Discovery, edited by M. Angel, Pergamon Press, pp. 15–37.
- Carmack, E.C., 1986. Circulation and mixing in ice-covered waters. In: The Geophysics of Sea Ice, edited by Understeiner N., Plenum, New York, pp. 641–741.
- Carmack, E.C. and T.D. Foster, 1974. Water masses and circulation in the Weddell Sea. In: Polar Oceans, edited by Dunbar, M.J., Arctic Inst. North Am., pp. 151–165.
- Craig, H., 1961. Standard for reporting concentrations of deuterium and oxygen-18 in natural waters. *Science*, **133**: 1833–1834.
- Craig, H. and L. Gordon, 1965. Deuterium and oxygen-18 variations in the ocean and the marine atmosphere. In: Stable Isotopes in Oceanographic Studies and Paleotemperatures, edited by Tongiorgi, E. and E. Cons, Naz. Delle Ric., Pisa (Italy), pp. 9–130.
- Deacon, G.E.R., 1937. The hydrography of the Southern Ocean. *Discov. Repts.*, **15**: 1–124.
- Deacon, G.E.R., 1979. The Weddell Gyre. *Deep-Sea Res.*, **26**: 981–995.
- Epstein, S. and T. Mayeda, 1953. Variation of $\delta^{18}\text{O}$ content of waters from natural sources. *Geochim. Cosmochim. Acta*, **4**: 213–224.
- Fahrbach, E., R.G. Peterson, G. Rohardt, P. Schlosser, and R. Bayer, 1994. Suppression of bottom water formation in the southeastern Weddell Sea. *Deep-Sea Res.*, **41**: 389–411.
- Fairbanks, R.G., 1982. The origin of continental shelf and slope water in the New York Bight and Gulf of Maine: Evidence from $\text{H}_2^{18}\text{O}/\text{H}_2^{16}\text{O}$ ratio measurement. *J. Geophys. Res.*, **87**: 5796–5808.
- Fofonoff, N.P., 1956. Some properties of seawater influencing the formation of Antarctic Bottom Water. *Deep-Sea Res.*, **4**: 32–35.
- Foldvik, A., T. Gammelsrod, and T. Torresen, 1985. Circulation and water masses of the southern Weddell Sea shelf. In: Oceanology of the Antarctic Continental Shelf, edited by Jacobs, S.S., *Am. Geophys. Union, Ant. Res. Ser.*, **43**: 5–20.
- Foster, T.D., 1972. An analysis of the cabbeling instability in sea water. *J. Phys. Oceanogr.*, **2**: 462–469.
- Frew, R.D., K.J. Heywood, and P.F. Dennis, 1995. Oxygen isotope study of water masses in the Prince Elizabeth Trough, Antarctica. *Mar. Chem.*, **49**: 141–153.
- Gill, A.E., 1973. Circulation and bottom water production in the Weddell Sea. *Deep-Sea Res.*, **20**: 111–140.
- Gordon, A.L., 1971. Oceanography of Antarctic Waters. In: Antarctic Oceanology I, edited by Reid, J.L., *Am. Geophys. Union, Ant. Res. Ser.*, **15**: 169–203.
- Gordon, A.L., 1975. An Antarctic oceanographic section along 170°E. *Deep-Sea Res.*, **22**: 357–377.
- Gordon, A.L., 1988. The southern ocean and global climate. *Oceanus*, **31**: 39–46.
- Gordon, A.L. and B.A. Huber, 1990. Southern Ocean winter mixed layer. *J. Geophys. Res.*, **95**: 11655–11672.
- Gordon, A.L. and W.D. Nowlin, 1978. The basin waters of the Bransfield Strait. *J. Phys. Oceanogr.*, **8**: 258–264.
- Gordon, A.L., C.T.A. Chen, and W.G. Metcalf, 1984. Winter mixed layer entrainment of Weddell Deep Water. *J. Geophys. Res.*, **89**: 637–640.
- Jacobs, S.S., R.G. Fairbanks, and Y. Horibe, 1985. Origin and evolution of water masses near the Antarctic continental margin: Evidence from $\text{H}_2^{18}\text{O}/\text{H}_2^{16}\text{O}$ ratios in seawater. In: Oceanology of the Antarctic Continental Shelf, edited by Jacobs, S.S., *Am. Geophys. Union, Ant. Res. Ser.*, **43**: 59–85.
- Khim, B.K. and D.E. Krantz, 1996. Oxygen isotopic identity of the Delaware Coastal Current. *J. Geophys. Res.*, **101**: 16509–16514.
- Khim, B.K., B.K. Park, and H.I. Yoon, 1997. Oxygen isotopic compositions of seawater in the Maxwell Bay of King George Island, West Antarctica. *Geosci. J.*, **1**: 115–121.
- Killworth, P.D., 1983. Deep convection in the world ocean. *Rev. Geophys. Space Phys.*, **21**: 1–26.
- Lehmann, M. and U. Siegenthaler, 1991. Equilibrium oxygen and hydrogen-isotope fractionation between ice and water. *J. Glaciol.*, **37**: 23–26.
- Mensch, M., R. Bayer, J.L. Bullister, P. Schlosser, and R.F. Weiss, 1996. The distribution of tritium and CFCs in the Weddell Sea during the mid-1980s. *Progr. Oceanogr.*, **38**: 377–415.
- Mosby, H., 1934. The waters of the Atlantic Antarctic Ocean. *Sci. Res. Norweg. Ant. Exped. 1927–1928*, **11**: 1–131.
- Orsi, A.H., W.D. Nowlin, and T. Whitworth, 1993. On the circulation and stratification of the Weddell Gyre. *Deep-Sea Res.*, **40**: 169–203.
- Ostlund, H.G. and G. Hut, 1984. Arctic Ocean water mass balance from isotope data. *J. Geophys. Res.*, **89**: 6373–6381.
- Schlosser, P., J.L. Bullister, and R. Bayer, 1991. Studies of deep water formation and circulation in the Weddell Sea using natural and anthropogenic tracers. *Mar. Chem.*, **35**: 97–122.
- Tan, F.C. and P.M. Strain, 1980. The distribution of sea-ice meltwater in the Eastern Canadian Arctic. *J. Geophys. Res.*, **85**: 1925–1932.
- Weiss, R.F., H.G. Ostlund, and H. Craig, 1979. Geochemical studies of the Weddell Sea. *Deep-Sea Res.*, **26**: 1093–1120.
- Whitworth, T. and W. Nowlin, 1987. Water masses and currents of the southern ocean at the Greenwich meridian. *J. Geophys. Res.*, **92**: 6462–6476.

Manuscript received August 13, 1997

Revision accepted March 4, 1998